Carbohydrate Polymers 87 (2012) 920–925

Contents lists available at ScienceDirect

Carbohydrate Polymers

journal homepage: www.elsevier.com/locate/carbpol

Short communication

# Synthesis and characterization of chitosan–PEG–Ag nanocomposites for antimicrobial application

K.S.V. Krishna Rao[a,b,*], P. Ramasubba Reddy[a], Yong-Ill Lee[b,**], Changdae Kim[c]

[a] Department of Chemistry, Yogi Vemana University, Kadapa 516 003, India
[b] Department of Chemistry, Changwon National University, Changwon, South Korea
[c] Department of Physics, Mokpo National University, Mokpo 534-729, South Korea

ARTICLE INFO

*Article history:*
Received 18 June 2010
Received in revised form 28 May 2011
Accepted 20 July 2011
Available online 28 July 2011

*Keywords:*
Chitosan
Poly(ethylene glycol)
Nanocomposite
Antimicrobial activity

ABSTRACT

New chitosan nanocomposites doped with silver nanoparticles were synthesized by a simple method. The chitosan particles were prepared by desolvation followed by crosslinking with poly(ethylene glycol-di-aldehyde), this was prepared with poly(ethylene glycol) in the presence of a silver nitrate solution. The developed nanocomposites were characterized using UV–visible, FTIR, XRD, TGA, SEM and TEM to understand their physico-chemical properties. These nanocomposites were shown to have anti bacterial activity towards *Escherichia coli*.

© 2011 Elsevier Ltd. All rights reserved.

## 1. Introduction

The design of metal nanoparticles/polymer composites has attracted much attention in the last few years, due to their wide range of applications, for example as catalysts and in the biomedical field (Barbucci, Consumi, Lamponi, & Leone, 2003). Many of these nanocomposites use a polymer as a stabilizer and supporting material. Considering the potential of such polymer composites for biological applications (Dornish, Aarnold, & Skaugrud, 1996), it is very surprising that the number of metal nanoparticle/bio-polymer networks reported so far is very limited. Indeed, this rare occurrence strongly contrasts with the abundance of published data on biopolymer network preparation in the pharmaceutical science literature (Peppas, 2004).

Certain medical applications of chitin require initial insolubility accompanied by a defined biodegradability of the polymer. This is the case, for instance, for wound dressings suitable for preventing tissue adhesion in internal surgery. These materials should ideally be insoluble when positioned in the surgical wound, and undergo progressive bio-erosion leading to complete resorption, as soon as they are no longer needed. Therefore, they should be enzymatically degradable (Jolle's & Muzzarelli, 1999; Muzzarelli, 1977, 1980). For development of chitosan gels the common and frequently used crosslinker is glutaraldehyde. This crosslinked material has subsequent application in biomedical field, such as enzyme immobilization and drug delivery(Giunchedi, Genta, Conti, Muzzarelli, & Conte, 1998; Zhu, Ma, Jia, Zhao, & Shen, 2009). Muzzarelli and coworkers documented the cytotoxic nature of this system and proposed different dialdehydes and polyaldehydes as crosslinkers. In this direction, many research groups have been using PEG dialdehydes and dicarboxylic acids as crosslinking agents in chitosan based biomaterials.

Among the bioactivity glycosaminoglycans, chitosan [1(4) 2-amino-2-deoxy-D-glucan] is a polyaminosaccharide, with good mechanical strength. They are acid-soluble deacetylated derivative of chitin obtained from *N*-deacetylation of chitin with strong alkali (Crescenzi & De Angelis, 1997). Chitin a naturally occurring polysaccharide, is found in the cuticles of arthropods, in the endoskeletons of cephalopods and fungi. Earlier studies reported that chitosan is bio-absorbable (Muzzarelli et al., 1988) and has good biocompatibility (Hirano & Noishiki, 1985). In addition, it has been demonstrated to be haemostatic (Malette, Quigley, Gaines, Johnson, & Rainer, 1983; Rao & Sharma, 1997) and bacteriostatic (Tarsi, Muzzarelli, Guzman, & Pruzzo, 1997). Moreover, it plays an important role in the cell regulation and tissue regeneration (Cho, Lee, & Song, 2005; Klokkevold, Vandemark, Kenney, & Bernard, 1996; Muzzarelli et al., 1989, 1993), it is a linear polyamine containing number of free amine groups that are readily available for crosslinking. Its cationic nature allows for ionic crosslinking with multivalent anions.

* Corresponding author at: Department of Chemistry, Yogi Vemana University, Kadapa 516 003, India. Tel.: +91 8562255410.
** Corresponding author at: Department of Chemistry, Changwon National University, Changwon, South Korea.
*E-mail addresses:* drksvkrishna@yahoo.com (K.S.V. Krishna Rao), yilee@cwnu.ac.kr (Y.-I. Lee).

0144-8617/$ – see front matter © 2011 Elsevier Ltd. All rights reserved.
doi:10.1016/j.carbpol.2011.07.028

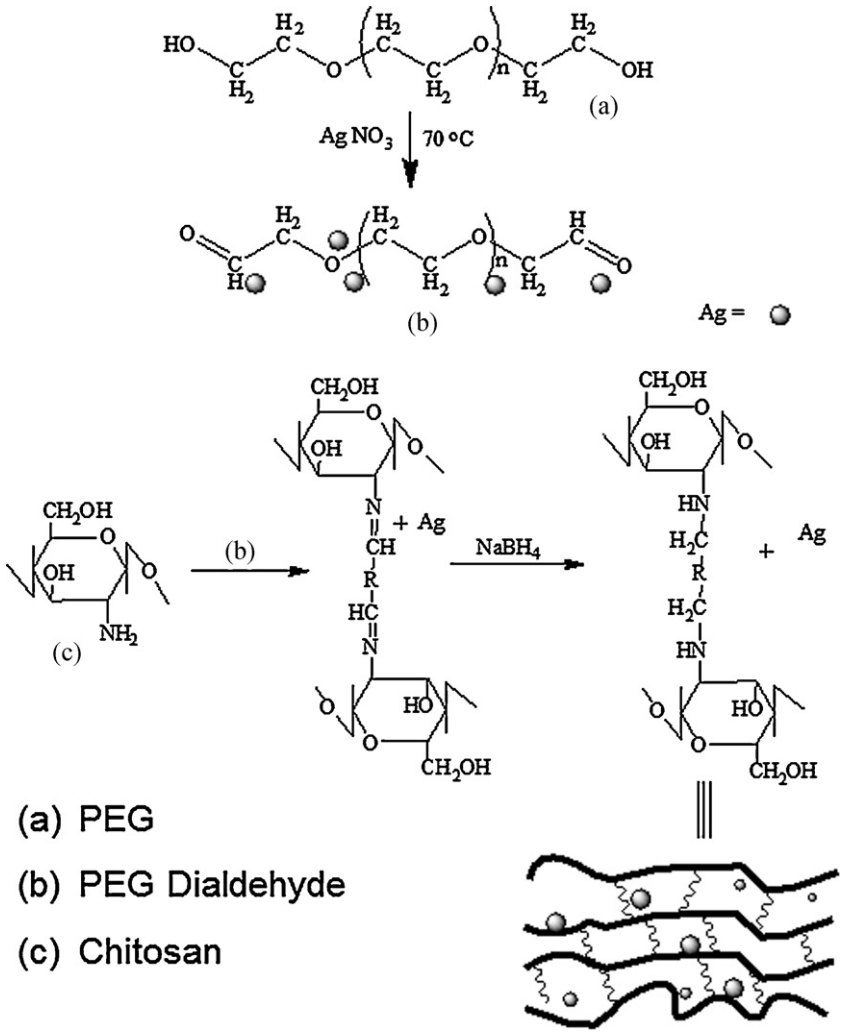


**Scheme 1.** Schematic representation of CS–PEG–Ag nanocomposite.

Recently Vimala et al. (2010) synthesized porous chitosan–silver nanocomposite membranes of 500 μm thickness which were crosslinked with glutaraldehyde for biomedical applications. In this present study, we prepared a novel nanocomposite, using silver nanoparticles CS–PEG as a polymeric shell. The morphology, thermal structure and characteristic of the CS–PEG–Ag were studied by UV, FTIR, XRD, TGA, SEM, and TEM. The CS–PEG–Ag nanocomposite has been investigation for its biocidal action against *Escherichia coli* (Scheme 1).

## 2. Materials and methods

### 2.1. Materials

Chitosan (CS) low molecular weight with 84% degree of deacetylation, sodium borohydrate ($NaBH_4$), silver nitrate ($AgNO_3$), poly(ethylene glycol) (Mw = 400), glacial acetic acid and ethanol were purchased from Aldrich Chemical Co. and used without further purification.

### 2.2. Preparation of chitosan nanogels

The Ag nanoparticles loaded chitosan nanogels were prepared by the one-step desolvation method. In brief, 0.25 g of chitosan was dissolved in 100 mL of 2% aqueous acetic acid and stirred overnight to obtain clear solution. The chitosan solution was desolvated by drop wise addition to 1000 mL of ethanol under constant stirring. After 5 min of stirring, 1 mL of freshly prepared poly(ethylene glycol) dialdehyde containing silver nanoparticles and catalytic quantities of HCl was added to crosslink the nanoparticles *in situ*. To this a catalytic amount of $NaBH_4$ was added to reduce silver ions into silver particles. This dispersion was stirred overnight until most of the ethanol was evaporated and then purified by centrifuging three times and redispersing in 30% ethanol in double distilled (DD) water. After the third centrifugation, the nanocomposite particles of chitosan–poly(ethylene glycol)–silver (CS–PEG–Ag) were redispersed in pure DD water (Scheme 1).

### 2.3. Fourier transform infrared spectroscopic studies

FTIR spectra were recorded on a Jasco, FTIR-430 (Japan). About 2 mg of the samples were ground thoroughly with KBr and pellets were prepared using a hydraulic press under a pressure of 600 kg/cm$^2$. Spectra were scanned between 500 and 4000 cm$^{-1}$.

### 2.4. UV–visible spectroscopy

UV–visible spectra of CS–PEG–Ag nanocomposite (10 mg in 1 mL of distilled water) were recorded on an Agilent 8453 UV spectrophotometer.

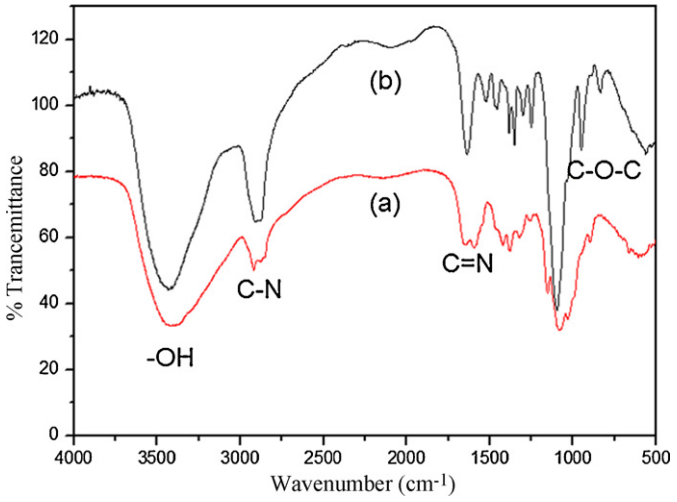


**Fig. 1.** FTIR spectra of chitosan (a) and PEG–CHO crosslinked CS (b).

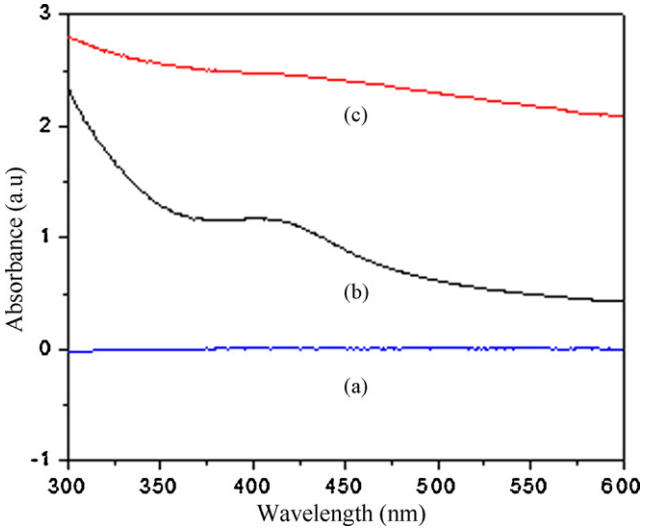


**Fig. 2.** UV–visible spectra of PEG (a), CS–PEG–Ag (b) and PEG–Ag nanocomposite (c).

### 2.5. X-ray diffraction (XRD) studies

Wide-angle X-ray diffractograms of CS–PEG–Ag nanocomposite was recorded on a Rigaku diffractometer (Philips, X'pert-PW3040) equipped with a Ni-filtered CuKά radiation (λ = 1.5418 Å). Samples were mounted on a sample holder and XRD scans were recorded in the angle range of 0–60° at the speed of 5°/min to estimate the crystallinity of the samples.

### 2.6. Thermogravimetric analysis

TGA curves of CS and CS–PEG–Ag nanocomposite were recorded using TA instruments sequential thermal analyzer (Model-SDT Q600, USA). Analysis of the samples was performed at heating rate of 10 °C/min under $N_2$ atmosphere at a purging rate of 100 mL/min.

### 2.7. Scanning electron microscopic (SEM) studies

The SEM images of nanocomposites were obtained by using a JSM-5610 (JEOL, Japan) Scanning Electron Microscope. Working distance of 10 mm was maintained and the acceleration voltage used was 5 kV with different magnification. CS–PEG–Ag nanocomposite were coated with gold by sputtering prior to measurements.

### 2.8. Transmission electron microscopic (TEM) study

Transmission electron microscopy images for CS–PEG–Ag nanocomposites were recorded using a JEM 2100F transmission electron microscope operating at an acceleration voltage of 15 kV. For TEM measurements, samples were prepared by dropping 10–20 μl of finely ground hydrogel solution on a copper grid and dried at room temperature.

### 2.9. Antibacterial activity

The antimicrobial activity of developed pure CS, CS–PEG–Ag nanocomposite (1 mg/mL and 2 mg/mL) against *Escherichia coli* (*E. coli*). The quantitative growth inhibition was measured by disc diffusion and LB broth method. Nutrient agar medium was prepared by mixing peptone (5.0 g), beef extract (3.0 g), and sodium chloride (5.0 g) in 1000 mL distilled water and the pH was adjusted to 7.0. Finally, agar (15.0 g) was added to the solution. The agar medium was sterilized in a conical flask at a pressure of 15 lbs for 30 min. This medium was transferred into sterilized petri-dishes in a laminar air flan. After solidification of the media, *E. coli* culture was streaked on the solid surface of the media. Nanocomposite solutions (10 mg/10 mL and 20 mg/10 mL distilled water) absorbed discs were placed on cultured agar plates (water used as control) and incubated for 12 h at 37 °C in the incubation chamber. At the end of the incubation period, the diameters of inhibition zones occurred on the medium were evaluated in millimeters.

In the LB broth method, 3.0 mL of the bacteria medium added into tubes contains different concentrations of nanocomposite solutions (10 mg/10 mL and 20 mg/10 mL distilled water), and the incubation was continued for 2 days. Culture with pure LB broth served as control. The bacterial viability was checked using their OD values by UV-visible spectrometer at 600 nm. The inhibition ratios for the CS–PEG–Ag were calculated as follows:

$$\text{Inhibition ratio}\quad (\%) = 100 - 100 \times \left(\frac{A_t - A_0}{A_{\text{con}} - A_0}\right)$$

where $A_0$ is the OD for bacterial broth medium before incubation; $A_t$ and $A_{\text{con}}$ are the ODs for nanocomposite and control sample after incubation, respectively.

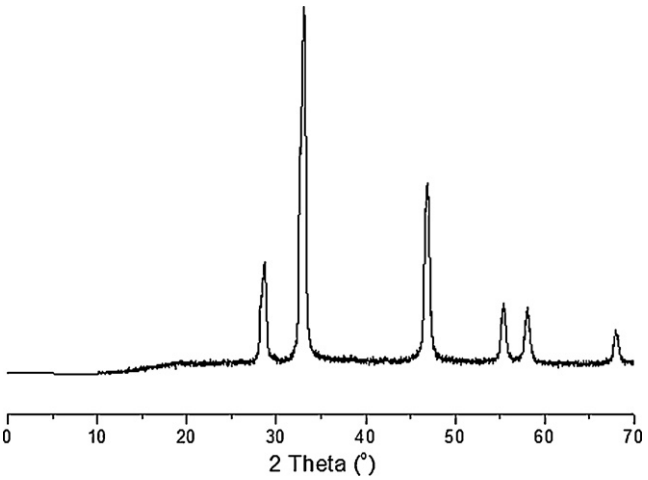


**Fig. 3.** XRD spectra of CS–PEG–Ag nanocomposite.

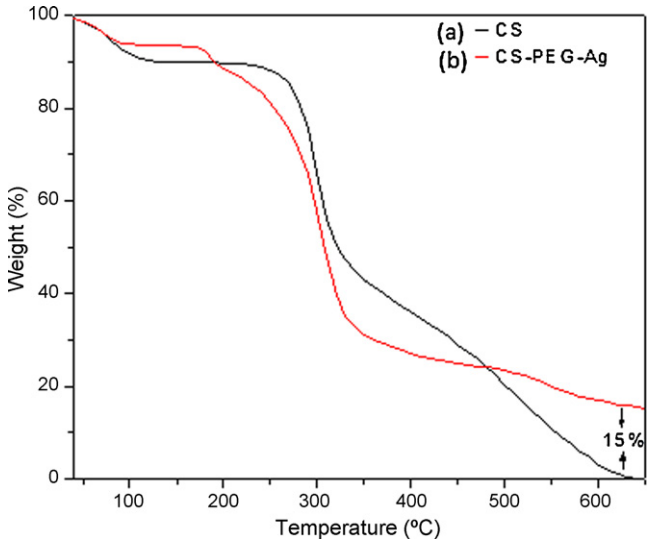


**Fig. 4.** TGA curves of CS (a) and CS–PEG–Ag (b) nanocomposite.

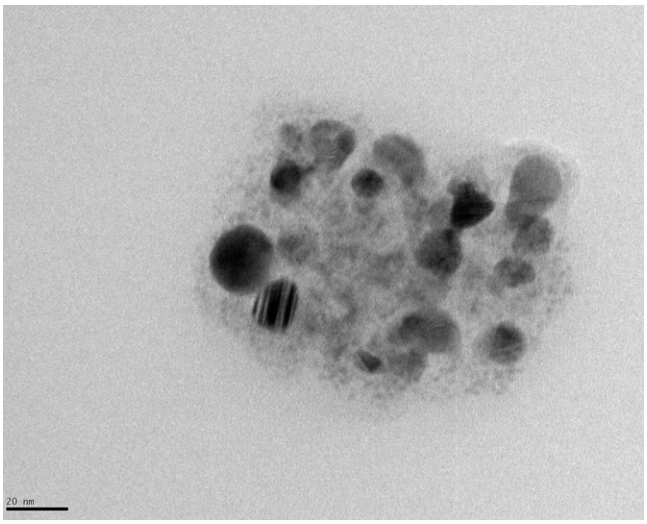


**Fig. 6.** Transmission electron microscopy image of CS–PEG–Ag nanocomposite.

## 3. Results and discussions

Fig. 1 shows the IR spectra of crosslinked CS and non-crosslinked CS. As like many organic compounds, CS presents a characteristic absorption in the IR domain. At 1650 $cm^{-1}$, its spectrum shows a band corresponding to an amide function, i.e., acetylated amine, whereas the band at 1590 $cm^{-1}$ corresponds to a free amine I function, i.e., deacetylated amine. When CS is chemically cross-linked with PEG aldehyde, the aldehyde reacts with the amine I functions to give a Schiff's base, creating covalent bridges between the polymer chains. The amide amount is not affected during crosslinking of CS, hence the band intensity at 1650 $cm^{-1}$ was considered as an internal reference. In contrast, intensity of the amine I band at 1590 $cm^{-1}$ is altered.

UV–visible spectroscopy is a valuable tool for structural characterization of silver nanoparticles. It is well known that the optical absorption spectra of metal nanoparticles are dominated by surface plasmon resonances (SPR), which shift to longer wavelengths with increasing particle size (Sosa, Noguez, & Barrera, 2003). The UV–visible spectra for all the preparations are shown in Fig. 2. All samples presented a minimum at ~320 nm that corresponds to the wavelength at which the real and imaginary parts of the dielectric function of silver almost vanish (Bradley, 1994). The sample with polymeric silver nanoparticles exhibited peaks ranging between 380 and 450, as shown in Fig. 2, which confirms the formation of silver nanoparticles.

Fig. 3 illustrates the X-ray diffraction patterns of CS–PEG–Ag nanocomposite. The diffractogram of CS–PEG–Ag nanocomposite is assigned to diffractions at $2\theta$ values of about 34°, 46°, 55° and 58° plane of face centered cubic (fcc) structure of silver nanoparticles. Such sharp peaks correspond to highly crystalline silver nanostructures formed in CS–PEG matrix.

TGA is important for formation and thermal stability of CS–PEG–Ag nanocomposite (Fig. 4). Starting decomposition temperature CS (303 °C) greater than CS–PEG–Ag nanocomposite (185 °C). In addition, a clear variation has been observed in TGA experiments in that CS–PEG–Ag nanocomposite exhibit better thermal stability than pure CS. The weight loss difference between the CS and CS–PEG–Ag nanocomposite is 15% represents the presence of silver nanoparticles (weight percent) in the CS–PEG–Ag nanocomposite.

Fig. 5 presents SEM micrographs of CS–PEG–Ag nanocomposites. This micrograph illustrates the formation of defined nanostructures of Ag in the CS–PEG matrices. This indicates that silver nanoparticles are formed along with the polymer chains rather than just Ag entrapment in the gel networks.

The properties of nanoparticles are strongly dependent upon their interactions with capping agent molecules (Kerker, 1985). Indeed, the surface chemistry of the nanoparticles can modify their interactions with external systems. TEM image of CS–PEG–Ag nanocomposite is presented in Fig. 6. TEM samples were prepared by dispersing the nanocomposite in deionized water by ultrasonication. A drop of this dispersion is taken on copper grids and

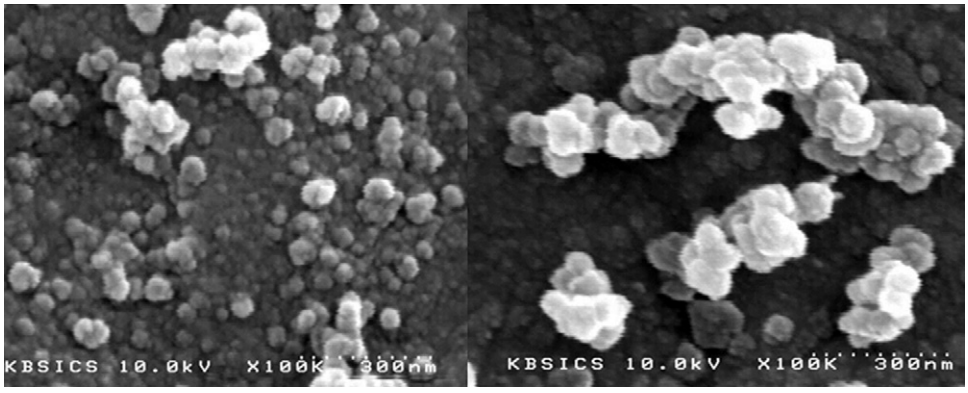


**Fig. 5.** SEM photograph of CS–PEG–Ag nanocomposite.

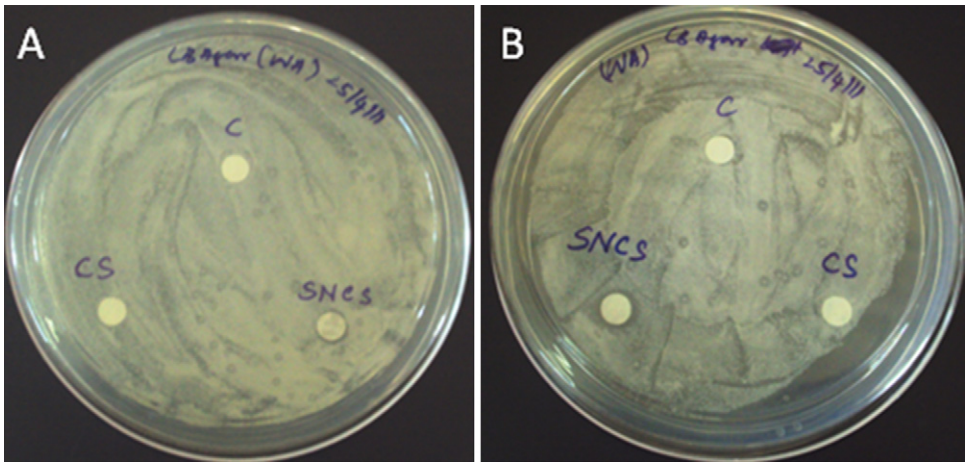


**Fig. 7.** Photograph of for 1 mg/mL sample (A) and for 2 mg/mL sample (B) on *Escherichia coli*. Abbreviations are 'C' is for control, 'CS' is for chitosan and 'SNCS' is for CS–PAG–Ag.

images were recorded. TEM images showed that the silver nanoparticles tend to be finely dispersed inside CS–PEG matrix.

TEM examination demonstrated that the sample is composed of metal core and polymer shell with multiple symmetry. Silver nanoparticles directly conjugated to CS–PEG matrix were synthesized in aqueous/ethanol solution. CS and PEG have oxygen- and nitrogen-bearing groups that can stabilize the nanoparticle surface. The strongest interactions with silver likely involve with oxygen and nitrogen. By using sodium borohydride, a strong reducing agent, CS–PEG matrix via direct bonding with these electron donor sites, and provides steric protection due to the network and bulkiness of the matrix. The optical signature of this sample can be better understood in terms of the distribution of sizes and shapes observed in the TEM.

Fig. 7 illustrates the antibacterial effect of pure chitosan and CS–PEG–Ag nanocomposite on *E. coli*. The results suggest that the CS–PEG–Ag nanocomposite showed a toxic effect on *E. coli* whereas pure chitosan does not involve much in the growth inhibition process. The antibacterial activity is due to the release of silver nanoparticles from CS–PEG–Ag nanocomposite. The diameter of growth inhibition zone is A (11 mm diameter for 2 mg/mL CS–PEG–Ag), which is greater than B (8 mm diameter for 2 mg/mL CS–PEG–Ag). LB broth medium is used for the quantitative determination of antimicrobial activity of CS, CS–PEG–Ag (1 mg/mL) and 2 mg/mL are shown in Fig. 8. The antibiotic ability to *E. coli*, expressed in terms as inhibition ratio, was enhanced with increasing concentration of silver nanocomposite. The maximum inhibition ratio is 88% (2 mg/mL CS–PEG–Ag) at 48 h. This preliminary study indicates that the polymer material composite CS–PEG–Ag can be used for antibacterial applications.

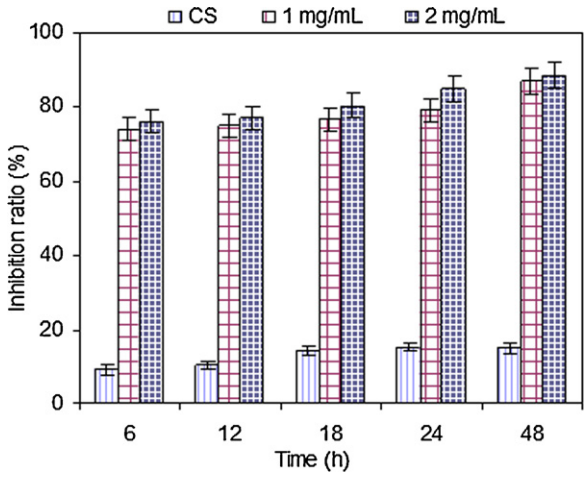


**Fig. 8.** Quantitative evaluation of inhibition ability to *E. coli* of pure CS, CS–PEG–Ag (1 mg/mL) and (2 mg/mL).

## 4. Conclusion

In conclusion, an easy and simple method has been developed for preparing CS–PEG–Ag nanocomposites. It is clearly illustrated that the silver nanoparticles are being formed not only on the surface of CS–PEG matrices but also throughout the networks. Nanocomposites are characterized using spectral, thermal, and electron microscopy methods. These nanocomposites showed good antibacterial activity towards *E. coli*.

## Acknowledgements

The authors gratefully acknowledge the support by Priority Research Centers Program through the National Research Foundation of Korea (NRF) funded by the Ministry of Education, Science and Technology (NRF 2010-0029634). And authors Dr. K.S.V.K. Rao and Mr. P.R.S. Reddy thank the Department of Science and technology (DST), New Delhi, India (DST No. SR/FT/CS-047/2009) for a financial support.

## References

Barbucci, R., Consumi, M., Lamponi, S., & Leone, G. (2003). Polysaccharides based hydrogels for biological applications. *Macromolecular Symposium*, *204*, 37–58.
Bradley, J. S. (1994). Clusters and colloids: From theory to applications. In G. E. Schmid (Ed.), *Clusters and colloids: From theory to applications* (pp. 459–536). Weinheim: VCH.
Cho, Y. W., Lee, J. R., & Song, S. C. (2005). Novel thermosensitive 5-fluorouracil-cyclotriphosphazene conjugates: Synthesis, thermosensitivity, degradability, and in vitro antitumor activity. *Bioconjugate Chemistry*, *16*, 1529–1535.
Crescenzi, V., & De Angelis, A. A. (1997). In R. A. A. Muzzarelli, & M. G. Peter (Eds.), *New chitosan chemical networks: Some synthetic procedures* (pp. 415–422). Italy: Chitin Handbook.
Dornish, M., Aarnold, M., & Skaugrud. (1996). Alginate and chitosan: Biodegradable biopolymers in drug delivery systems. *European Journal of Pharmaceutical Sciences*, *4*, 153.
Hirano, S., & Noishiki, Y. (1985). The blood compatibility of chitosan and N-acylchitosans. *Journal of Biomedical Material Research*, *19*, 413–417.
Jolle's, P., & Muzzarelli, R. A. A. (Eds.). (1999). *Chitins and chitinases*. Basel: Birkhauser.
Kerker, M. (1985). The optics of colloidal silver: Something old and something new. *Journal of Colloid and Interface Science*, *105*, 297–314.
Klokkevold, P. R., Vandemark, L., Kenney, E. B., & Bernard, G. W. (1996). Osteogenesis enhanced by chitosan (poly N-acetyl glucosaminoglycan) in vitro. *Journal of Periodontology*, *67*, 1170–1175.
Malette, W. G., Quigley, H. J., Gaines, R. D., Johnson, N. D., & Rainer, W. G. (1983). Chitosan, a new haemostatic. *Annals of the Thoracic Surgery*, *36*, 55–61.
Muzzarelli, R. A. A. (1977). *Chitin*. Oxford: Pergamon Press., p. 140.

Muzzarelli, R. A. A. (1980). Immobilization of enzymes on chitin and chitosan. *Enzyme and Microbial Technology*, *2*, 177–184.
Muzzarelli, R., Baldassarre, V., Conti, F., Ferrara, P., Biagini, G., & Gazzanelli, G. (1988). *Biomaterials*, *9*, 247–252.
Muzzarelli, R. A. A., Biagini, G., Bellardini, M., Simonelli, L., Castaldini, C., & Fratto, G. (1993). Osteoconduction exerted by methylpyrrolidinonechitosan used in dental surgery. *Biomaterials*, *14*, 39–43.
Muzzarelli, R. A. A., Biagini, G., Pugnaloni, A., Filippini, O., Baldassarre, V., & Castaldini, C. (1989). Reconstruction of parodontal tissue with chitosan. *Biomaterials*, *10*, 598–603.
Giunchedi, P., Genta, I., Conti, B., Muzzarelli, R. A. A., & Conte, U. (1998). *Biomaterials*, *19*, 157–161.
Peppas, N. A. (2004). Devices based on intelligent biopolymers for oral protein delivery. *International Journal of Pharmaceutics*, *277*, 11–17.
Rao, S. B., & Sharma, C. P. (1997). Use of chitosan as a biomaterial: Studies on its safety and hemostatic potential. *Journal of Biomedical Material Research*, *34*, 21–28.
Sosa, I. O., Noguez, C., & Barrera, R. G. (2003). Optical properties of metal nanoparticles with arbitrary shapes. *Journal of Physical Chemistry*, *107*, 6269–6275.
Tarsi, R., Muzzarelli, R. A. A., Guzman, C. A., & Pruzzo, C. (1997). Inhibition of *Streptococcus mutans*. Adsorption to hydroxyapatite by low molecular-weight chitosans. *Journal of Dental Research*, *76*, 665–672.
Vimala, K., Mohan, Y. M., Sivudu, K. S., Varaprasad, K., Ravindra, S., Reddy, N. N., et al. (2010). Fabrication of porous chitosan films impregnated with silver nanoparticles: A facile approach for superior antibacterial application. *Colloids and Surfaces B: Biointerfaces*, *76*, 248–258.
Zhu, L., Ma, J., Jia, N., Zhao, Y., & Shen, H. (2009). Chitosan-coated magnetic nanoparticles as carriers of 5-fluorouracil: Preparation, characterization and cytotoxicity studies. *Colloids and Surfaces B: Biointerfaces*, *68*, 1–6.